ELSEVIER

Soil Dynamics and Earthquake Engineering 27 (2007) 1000–1011

SOIL DYNAMICS AND EARTHQUAKE ENGINEERING

www.elsevier.com/locate/soildyn

Non-stationary random vibrations of a shear beam under high frequency seismic effects

Zbigniew Zembaty*

Faculty of Civil Engineering, Opole University of Technology, ul, Mikolajczyjka 5, 45-271 Opole, Poland

Received 30 August 2006; received in revised form 13 February 2007; accepted 12 March 2007

Abstract

Band-limited, non-stationary random vibrations of a shear beam are studied in order to investigate high frequency seismic effects on building structures. A solution for the evolutionary spectral density of the shear beam response to a time segment of band-limited white noise is given in a closed form. The root mean square (rms) and peak response of the shear beam are studied for two characteristic frequency bands: the conventional 1–4 Hz and higher frequency 4–16 Hz, characteristic for rockburst ground motion. Applying the criterion of equal excitation intensity with constant rms velocity, both responses are analyzed in detail and compared. The "switching off" fundamental mode for high frequency excitations results in characteristic overshoot of the stationary response level by the non-stationary rms response and an amplification of the response in the upper part of the shear beam.

Keywords: Seismic engineering; Non-stationary random vibrations; Peak response; Rockbursts; Shear beams

1. Introduction

Typical seismic effects which can affect civil engineering structures derive from earthquakes which dominate in the frequency band 0–5 Hz and decrease to zero at about 10 Hz (see e.g. acceleration records from the database by Ambraseys et al. [1]). In some situations e.g. of a shallow focus and near-field record, particular site geology or for vertical seismic components this upper limit can be extended, sometime even up to 20 Hz.

However, the structural foundations can be subjected to kinematic motions also from artificial or semi-artificial seismic effects like:

- rockbursts,
- nuclear underground explosions,
- distant conventional explosions (e.g. from surface mining, quarries),
- close (to structure) explosions of underground ammunition storages,
- pile hammering,
- traffic ground motion, etc.

These sources of seismic vibrations differ primarily in the energy released. Depending on the source-to-site distance ranging from tens of metres to tens of kilometres, the actual, generated ground motion may substantially differ because various frequency bands attenuate differently in the ground [2,3]. Fig. 1 presents characteristic frequency bands of surface accelerations for various sources of seismic ground motions. The lightly shaded areas show less likely frequencies to contribute and highlight the approximate character of the presented diagram.

Though excitations deriving from these artificial sources of seismic excitations result usually in low level vibrations and (with few exceptions) cause only minor structural damage, most of these effects occur much more frequently than natural earthquakes and often generate human discomfort as well as induce strong equipment response. And since they differ qualitatively from natural seismic vibrations they are worth further detailed studies. Indeed, as the frequency content of excitations increases, the resulting structural motion departs more and more from

*Tel.: +48 602 183 655; fax: +48 77 4 566 124.
E-mail address: zet@po.opole.pl.
URL: http://www.zet.po.opole.pl.

0267-7261/$ - see front matter © 2007 Elsevier Ltd. All rights reserved.
doi:10.1016/j.soildyn.2007.03.003

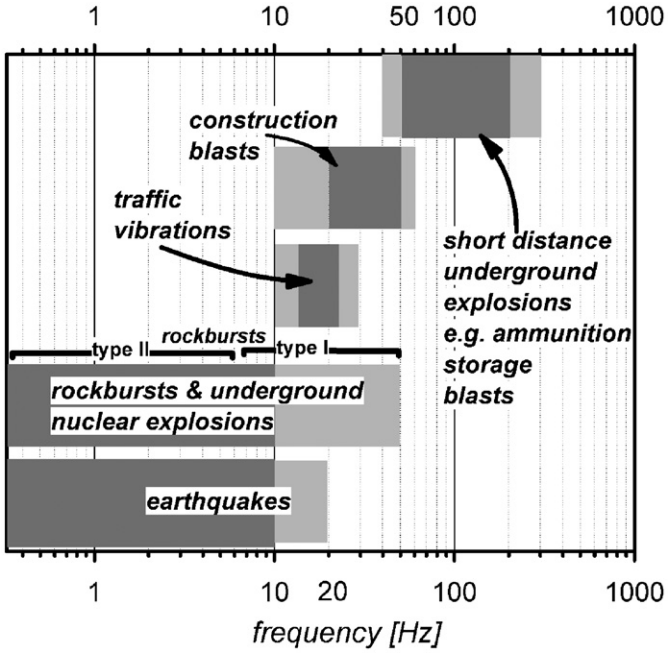

Fig. 1. A diagram showing frequency bands of various natural and artificial seismic excitations.

classic seismic vibrations. Thus some conclusions based on classic seismic engineering may even be misleading. As an example one can give a particularly difficult problem of quantitative measures of seismic intensity, still ambiguous even for natural earthquakes (e.g. [4,5]) or a question how to assess ground motion intensity from blasts. The latter one may be of serious financial importance when determining the origin of so-called cosmetic cracks in the buildings around an underground mine or a quarry.

While the classic, natural seismic effects on structures are extensively studied, the structural effects caused by seismic excitations with higher frequency contents are subject of detailed analyses only in very few papers (e.g. [6,7]) or more general analyses in practical context of construction vibrations or surface mining [8]. These analyses were carried with the application of deterministic models of structural vibrations. In present paper this problem is studied in terms of non-stationary random vibrations and peak response of a uniform shear beam. This type of dynamic system represents a specific, simplified model of a multistory building, a principal object of interests of seismic engineering codes.

2. Rockburst induced seismic effects versus natural earthquakes

Rockbursts, together with reservoir induced ground quakes, belong to a wider phenomenon of ground failures caused by human activity. In spite of their artificial origin they produce seismic events random with respect to time and intensity and in a limited sense also with respect to place of their origin. The strongest rockbursts may reach magnitude similar to small earthquakes (M_L close to 5) and are collected by the USGS National Earthquake Information Center in Denver (http://neic.usgs.gov) from data gathered by the world network of seismograph stations. Such strong quakes are subjects of careful studies to differentiate them from underground nuclear explosions. This research, concentrated on teleseismic epicentral distances (>2000 km), is sponsored by various governmental and international organizations to secure proper implementation of the Nuclear Test Ban Treaty [9].

The energy generated underground by a strong rockburst can be similar to an underground nuclear blast or a small earthquake. However, when comparing the acceleration records of rockbursts and earthquakes some differences between them appear to be not only quantitative but also qualitative. After collecting extensive database of rockburst induced surface and structural vibrations in the "LGOM" copper basin in South-West Poland, these differences were identified and analyzed in numerous research reports and summarized in a recent paper [10]. This study divided the rockbursts into two characteristic types:

- Events of type I with rather low intensity, return period of 3–6 months, very short duration (1–2 s), and Fourier spectra shifted to higher frequencies (about 20–40 Hz) similar to strong surface explosion effects [8].
- Rare events of type II (return period of a few years), longer duration (about 5 s or more) and dominating part of Fourier spectra below 5–10 Hz similar to weak, shallow earthquakes.

Independent geophysical analyses (e.g. [11]) confirm that this classification has some seismological reasoning, ascribing the type I events to routine mining activity while the second ones are only loosely correlated with the ore exploitation or even can be small earthquakes triggered in the nearby faults by the mine activity.[1] In Fig. 2a,b typical acceleration time history records of both types of these events are shown. In Fig. 2e respective Fourier spectra of the two accelerograms together with an averaged Fourier spectrum of typical earthquakes [12] are plotted. In spite that the peak ground acceleration (PGA) of the event type I reached 101 cm/s^2 it did not result in any damages, while the event of type II with PGA = 70 cm/s^2 caused some damages to buildings in the nearby town: cracks between panels in prefabricated, 10-story buildings, damage to the counter-weight of an elevator and some minor damages to brick masonry buildings. It is interesting to note that this destructive capacity of the event type II is reflected in the respective velocity time histories in the two analyzed cases (Fig. 2c,d). The peak ground velocity (PGV) for type II event equaled about 6.2 cm/s while respective PGV for the event type I equaled about 2.5 cm/s. The role of velocity as a much better measure of destructive capacity of seismic excitations is known for a long time and is explained

[1] M.D. Trifunac personal communication.

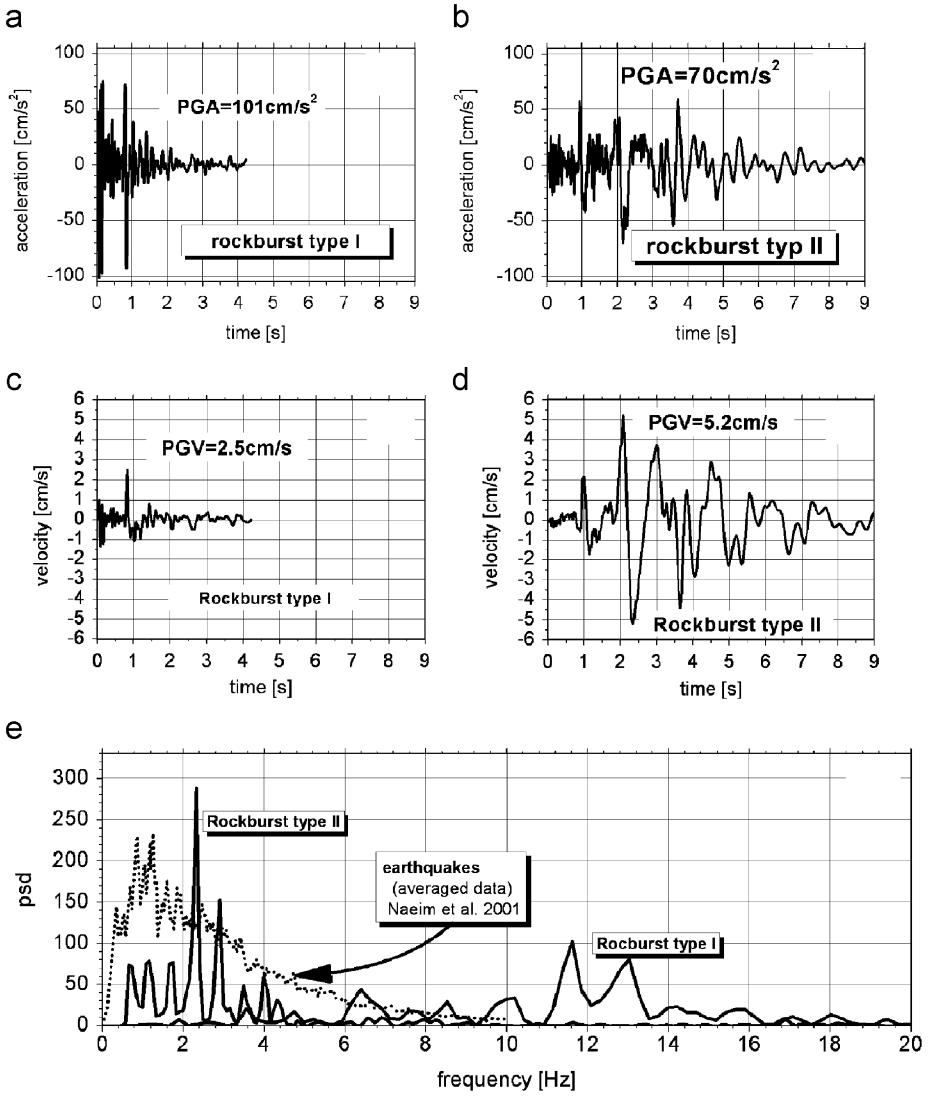

Fig. 2. Horizontal accelerations (a,b) and velocities (c,d) as well as Fourier spectra of natural earthquakes [12] and two records of rockbursts (e). Type I: ("*Sosnowa*" station—February 2nd 2001); type II: ("*Hubala*" station—February 20th 2002).

heuristically by a direct correlation between velocity and kinetic energy induced in the structure [8]. Looking at Fig. 2e one can notice that the main difference between the two records can be explained by their frequency content. What is more, by simply shifting their scale in frequency domain one can change event type II into type I and vice versa. Doing this, obviously changes the intensity of these records. But when accepting the idea of the same intensity for constant PGV, both records can be scaled appropriately.

3. Shear beam structural model and stochastic process representation of high frequency seismic effects

The structural response to excitations of type II events can be analyzed using conventional methods of seismic engineering, noting their rather short duration (about 5 s) in comparison to typical natural earthquakes (about 15–30 s). Some earthquakes, however, also represent short durations (<5 s) making their records almost identical to type II rockbursts. When it comes to the type I events their effects on structures are quite different. The natural frequencies of the first vibration mode of typical civil engineering structures, particularly multistory buildings, usually stay below 5 Hz. For example an engineering rule of thumb makes it possible to assess the lowest natural period of 10-story building as equal to 1 s (1 Hz) or 0.1 s for a 1-story building (10 Hz) and interpolate natural periods for the intermediate number of stories. Therefore the shift of a dominating frequency band from 1–5 Hz to about 5–20 Hz (compare Fig. 2e) leads to excitations of higher natural modes. The unique features of such a structural response derive not only from the presence of these higher vibration modes but rather from the lack of the fundamental mode(s) in the overall seismic vibrations. To capture only the essential effects differing higher frequency vibrations from the conventional ones, the simplest possible model should be applied, apart from the single

degree of freedom systems (SDOF) as they do not account for the presence of various natural vibration modes. Such a simple structural model can be found among so-called shear beams which can represent various types of engineering systems, e.g. tall buildings, dams, or soil profiles.

Consider a shear beam shown schematically in Fig. 3a. The equation of motion of such a uniform cantilever shear beam under horizontal seismic excitations $u(t)$ takes the following form:

$$m\frac{\partial^2 q}{\partial t^2}+c_1\frac{\partial q}{\partial t}+c_2K\frac{\partial^3 q}{\partial z^2\partial t}-K\frac{\partial^2 q}{\partial z^2}=-m\ddot{u}(t), \tag{1}$$

in which K is its shear stiffness, m represents mass per unit length and c_1 stands for so-called coefficient of external damping while c_2 represents internal (material damping). Dividing both sides of Eq. (1) by m leads to the following, normalized form of the shear beam equation of motion:

$$\frac{\partial^2 q}{\partial t^2}+\frac{c_1}{m}\frac{\partial q}{\partial t}+c_2c_S^2\frac{\partial^2 q}{\partial z^2}-c_S^2\frac{\partial^2 q}{\partial z^2}=-\ddot{u}(t), \tag{2}$$

where $c_S=\sqrt{(K/m)}$ represents velocity of shear waves propagating along the beam. As shear beams deflect only in shear, their natural frequencies occur in a uniform sequence, similar to the sequence of the natural frequencies of a tall building (Fig. 3b) and what is also very important both, the natural frequencies ω_j and modes ψ_j can be written in closed form solutions:

$$\omega_j=(2j-1)\frac{\pi c_S}{2H}, \tag{3}$$

$$\psi_j(z)=\sin\left(\frac{\omega_j z}{c_S}\right). \tag{4}$$

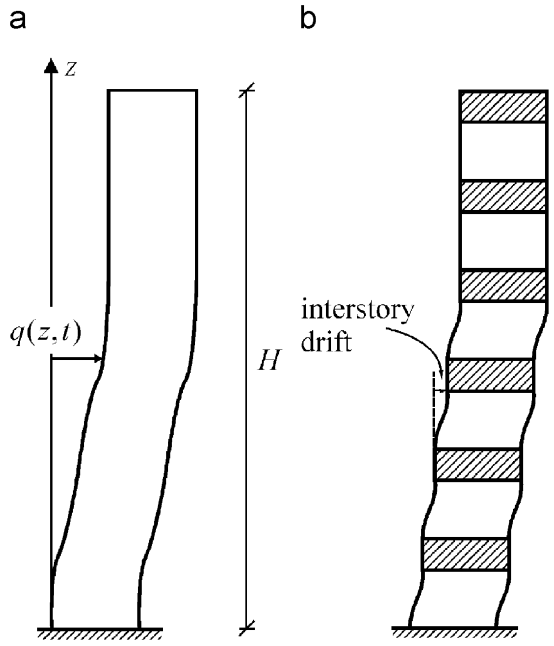

Fig. 3. A shear beam model of a multistory building.

In Eq. (3) H stands for the height of the shear beam from Fig. 3. The shear beams or shear plates as models of multistory buildings were subjects of the research by Todorovska and Trifunac [13], Todorovska and Lee [14] and Safak [15]. Although the shear beam seems quite simplistic as a building model, it allowed to analyze complicated shear wave propagation effects not possible to explain by the traditional finite element approach commonly used in seismic engineering. In 1997 Iwan [16] published a paper in which he proposed a new format of response spectrum, the so-called *drift spectrum* which was based on the measures of maximum drift of a cantilever shear beam under seismic excitations. Since the interstory drift (Fig. 3b) is also a good measure of destructive effects of earthquakes on multistory buildings it is often applied in seismic building codes. The Iwan's drift spectrum [16] was proposed as a specific measure of demand of earthquake ground motion in the near-field regions of excitations. Although the shear beam is a rather simple structural model its seismic response is in good agreement with complicated finite element analyses of buildings making it a very convenient structural model as it captures specific dynamic properties of high buildings while it is still relatively simple in numerical analyses. In 1999 Chopra and Chintanapakdee [17] showed that the choice of the shear beam as a good structural model did not depend on the type of seismic excitations, while in 2006 Sasani et al. [18] improved the shear beam wave propagation model to properly account for dispersive type of damping.

To carry out more general analyses, independent from the recorded time history and structural type, a model of the excitation process in form of a random process will be applied. Two unique features of the ground motion should be accounted for:

- short duration, requiring the transient effects to be included,
- the specific spectral content of the excitations.

Consider a stationary pulse of band-limited white noise (Fig. 4a) with spectral intensity S_0. The non-stationary structural response to such excitations properly models the strongest non-stationarity possible to be present in seismic vibrations. The white noise excitations switch on at $t=0$ and switch off after t_0 seconds. Under such excitations the structural response builds up until $t=t_0$ and then falls to zero. To compare structural vibrations with excitations from different frequency bands and still keep approximately the same intensity level, the constant PGV criterion is usually applied (see e.g. [7]). For the purpose of this analysis, when the shift in the frequency band is not substantial (Fig. 2) the constant intensity criterion can be applied approximately by keeping constant root mean square (rms) velocity of excitations. In fact the constant peak velocity as a criterion of constant intensity is only very approximate, experimental rule not always totally holding in seismic engineering (see e.g. [4]). Under this

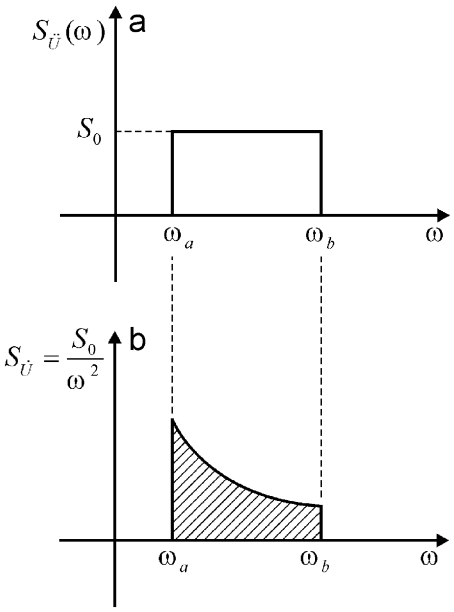

Fig. 4. Band-limited white noise spectrum of the excitation, acceleration process (a) as well as the respective spectrum of excitation velocity.

assumption the frequency band from ω_a to ω_b can be changed only if the respective rms excitation velocity is kept constant, which for stationary random processes means:

$$\int_{\omega_a}^{\omega_b} S_V \,\mathrm{d}\omega = \int_{\omega_a}^{\omega_b} \frac{S_{\ddot{U}}}{\omega^2}\,\mathrm{d}\omega = \int_{\omega_a}^{\omega_b} \frac{S_0}{\omega^2}\,\mathrm{d}\omega = S_0\left[\frac{1}{\omega_a} - \frac{1}{\omega_b}\right] = \text{const}, \tag{5}$$

where S_V stands for spectral density of excitation velocity. The unique features of the high frequency seismic excitations of structures appear then in switching on and off various natural modes of Eqs. (3) and (4) while changing frequency band (ω_a; ω_b), (Fig. 4a) and keeping constant intensity (equal area of Fig. 4b).

4. Random vibrations of cantilever shear beam under non-stationary excitations

Consider now solution of equation of motion of the shear beam from Fig. 3a (Eq. (2)) in form of familiar modal superposition:

$$q(z,t) = \sum_{j=1}^{\infty} \psi_j(z) Q_j(t) \tag{6}$$

in which $\psi_j(z)$ stands for modal shapes given by formula (4) and $Q_j(t)$ represents vibrations of the beam in normal coordinates. Substituting the normal expansion (6) into Eq. (2) and taking into account orthogonal properties of eigenmodes assumed to hold also with respect to damping coefficients gives

$$\ddot{Q}_j + \left(\frac{c_1}{m} + c_2 c_S^2 \omega_j^2\right)\dot{Q}_j + \omega_j^2 Q_j = -a_j \ddot{u}(t), \quad j = 1,2,3,\ldots, \tag{7}$$

where a_j denotes modal participation factor

$$a_j = \frac{\int_0^H \psi_j(z)\,\mathrm{d}z}{\int_0^H \psi_j^2(z)\,\mathrm{d}z}. \tag{8}$$

Introducing damping ratio of the jth mode defined as

$$\xi_j = \frac{\chi}{2\omega_j} + \frac{\kappa\omega_j}{2}, \tag{9}$$

makes it possible to write Eq. (7) in the standard format of SDOF system

$$\ddot{Q}_j + 2\xi_j\omega_j\dot{Q}_j + \omega_j^2 Q_j = -a_j\ddot{u}(t), \quad j = 1,2,3,\ldots. \tag{10}$$

The new damping coefficients from Eq. (9)

$$\chi = \frac{c_1}{m}, \tag{11}$$

$$\kappa = c_2 c_S^2 \tag{12}$$

represent two types of damping [19]: the mass proportional damping in which case

$$\xi_j = \frac{\chi}{2\omega_j} \quad (\kappa = 0), \tag{13}$$

and stiffness proportional, respectively,

$$\xi_j = \frac{\kappa\omega_j}{2} \quad (\chi = 0). \tag{14}$$

If both χ and κ are not equal to zero then ξ_j is given by Eq. (9) and the combined modal damping is applied. Each of these three damping models makes it possible to decouple modal responses. However, numerous experiments in real scale have shown that all of them still leave a lot to be desired. A preference should only be given to the stiffness proportional damping as most of the experiments indicate an increase in modal damping with increasing frequency.

Substituting respective Duhamel's integrals solving Eqs. (7) into the modal expansion (6) yields

$$q(z,t) = -\sum_{j=1}^{\infty} \psi_j(z) a_j \int_0^t \ddot{u}(t-\tau) h_j(\tau)\,\mathrm{d}\tau, \tag{15}$$

where $h_j(t)$ are modal impulse response functions:

$$h_j(t) = \frac{1}{\omega_{jd}} \mathrm{e}^{-\xi_j\omega_j t}\sin(\omega_{jd}t), \quad \omega_{jd} = \omega_j\sqrt{1-\xi_j^2}. \tag{16}$$

Assume now that the horizontal accelerations are modeled by a non-stationary random process with zero mean and spectral representation which can be written in format of the following Stieltjes–Fourier representation [20]:

$$\ddot{u}(t) = \int_{-\infty}^{\infty} A(t,\omega)\mathrm{e}^{\mathrm{i}\omega t}\,\mathrm{d}\hat{\ddot{u}}(\omega) \tag{17}$$

in which $A(t,\omega)$ is a deterministic modulating function, $\mathrm{i} = \sqrt{(-1)}$, symbol $\hat{\ddot{u}}(\omega)$stands for random function with

orthogonal increments i.e.:

$$\langle d\hat{\ddot{u}}(\omega_1) d\hat{\ddot{u}}^*(\omega_2)\rangle = \begin{cases} \langle |d\hat{\ddot{u}}(\omega)|^2\rangle = S_{\ddot{u}}(\omega)\,\mathrm{d}\omega & \text{for } \omega_1 = \omega_2 = \omega, \\ 0 & \text{for } \omega_1 \neq \omega_2 \end{cases} \tag{18}$$

and symbol $\langle\ \rangle$ stands for operator of the mathematical expectation.

The Priestley's spectral representation (17) can be interpreted as the decomposition of the excitation process onto a series of modulated harmonics in both time and frequency domains. For uniformly modulated process i.e. when $A(t,\omega) = A(t)$ formula (17) reduces to

$$\ddot{u}(t) = \int_{-\infty}^{\infty} A(t,\omega)\mathrm{e}^{\mathrm{i}\omega t}\,\mathrm{d}\hat{\ddot{u}}(\omega) = A(t)\int_{-\infty}^{\infty}\mathrm{e}^{\mathrm{i}\omega t}\,\mathrm{d}\hat{\ddot{u}}(\omega) = A(t)\tilde{\ddot{u}}(t) \tag{19}$$

with tilde~denoting stationary process. When $A(t,\omega) = 1 =$ const then the analyzed process reduces to the stationary one i.e. $\ddot{u}(t) = \tilde{\ddot{u}}(t)$.

Substituting spectral representation (17) into the eigen-series solution (15) gives response displacements

$$q(t,z) = \sum_{j=1}^{\infty} a_j\psi_j(z)\int_{-\infty}^{\infty} M_j(t,\omega)\,\mathrm{e}^{\mathrm{i}\omega t}\,\mathrm{d}\hat{\ddot{u}}(\omega) \tag{20}$$

in terms of response modulating functions:

$$M_j(t,\omega) = \int_0^t h_j(\tau)A(t-\tau,\omega)\mathrm{e}^{-\mathrm{i}\omega\tau}\,\mathrm{d}\tau \tag{21}$$

and impulse response functions $h_j(t)$ as well as the excitation modulating function $A(t,\omega)$. When one considers the excitation as stationary process switching "on" and "off", as it was already assumed in the previous section, the modulating function $A(t,\omega)$ simplifies to a "box-car" form:

$$A = A(t) = \begin{cases} 0 & \text{for } t<0, \\ 1 & \text{for } 0<t<t_0, \\ 0 & \text{for } t>t_0. \end{cases} \tag{22}$$

In this case integral (21) can be calculated in closed form and equals:

$$M_j(t,\omega) = \begin{cases} 0 & \text{for } t<0, \\ H_j(\omega)[1-P_j(t,\omega)] & \text{for } 0<t<t_0, \\ H_j(\omega)[P_j(t-t_0,\omega)-P_j(t,\omega)] & \text{for } t>t_0, \end{cases} \tag{23}$$

where

$$P_j(t,\omega) = \frac{1}{\omega_{jd}}\mathrm{e}^{-\xi_j\omega_j t}(\cos\omega t - \mathrm{i}\sin\omega t) \times [(\xi_j\omega_j + \mathrm{i}\omega)\sin\omega_{jd}t + \omega_{jd}\cos\omega_{jd}t] \tag{24}$$

while $H_j(\omega)$ is the modal frequency response function

$$H_j(\omega) = [\omega_j^2 - \omega^2 + 2\mathrm{i}\xi_j\omega_j\omega]^{-1}. \tag{25}$$

Eq. (20) together with the orthogonal property (18) can now be used to calculate any response statistics of the response process. For example the mean square displacements along the height of the shear beam equals:

$$\sigma_q^2(z,t) = \sum_{j=1}^{\infty}\sum_{k=1}^{\infty} a_j a_k\psi_j(z)\psi_k(z) \times \int_{-\infty}^{\infty} M_j(t,\omega)M_k^*(t,\omega)S_{\tilde{\ddot{u}}}(\omega)\,\mathrm{d}\omega, \tag{26}$$

where $S_{\tilde{\ddot{u}}}(\omega)$ denotes classic, stationary spectral density of the stationary process $\tilde{\ddot{u}}(t)$ "associated" with the non-stationary one (both processes coincide when $A(t,\omega) = 1$), while the integrand of Eq. (26) represents evolutionary spectral density of the response:

$$S_q(z,t,\omega) = \sum_{j=1}^{\infty}\sum_{k=1}^{\infty} a_j a_k\psi_j(z)\psi_k(z)M_j(t,\omega)M_k^*(t,\omega)S_{\tilde{\ddot{u}}}(\omega). \tag{27}$$

By noting that the shear force along the shear beam equals $F(z) = K\partial q/\partial z$, it is easy to formulate equations analogous to Eqs. (19) and (20) representing mean square response and evolutionary spectral density of shear forces along the beam height:

$$\sigma_F^2(z,t) = K^2\sum_{j=1}^{\infty}\sum_{k=1}^{\infty} a_j a_k\frac{\partial\psi_j(z)}{\partial z}\frac{\partial\psi_k(z)}{\partial z} \times \int_{-\infty}^{\infty} M_j(t,\omega)M_k^*(t,\omega)S_{\tilde{\ddot{u}}}(\omega)\,\mathrm{d}\omega, \tag{28}$$

$$S_F(z,t,\omega) = K^2\sum_{j=1}^{\infty}\sum_{k=1}^{\infty} a_j a_k\frac{\partial\psi_j(z)}{\partial z}\frac{\partial\psi_k(z)}{\partial z} \times M_j(t,\omega)M_k^*(t,\omega)S_{\tilde{\ddot{u}}}(\omega). \tag{29}$$

when the excitation process is stationary, then also the response is stationary, the integration limits in Eq. (21) are infinite and $M_j(t,\omega)$ become modal frequency response functions:

$$H_j(\omega) = \left[\omega_j^2 - \omega^2 + 2\mathrm{i}\xi_j\omega_j\omega\right]^{-1}. \tag{30}$$

By moving the summation operator from Eqs. (26)–(29) into Eq. (21) one can obtain alternative form of mean square response:

$$\sigma(z,t) = \int_{-\infty}^{\infty} M(z,t,\omega)M^*(z,t,\omega)S_{\tilde{\ddot{u}}}(\omega)\,\mathrm{d}\omega \tag{31}$$

with

$$M(z,t,\omega) = \begin{cases} M_q(z,t,\omega) = \sum_{j=1}^{\infty} a_j\psi_j(z)\int_0^t h_j(\tau)A(t-\tau,\omega)\mathrm{e}^{-\mathrm{i}\omega\tau}\,\mathrm{d}\tau & \text{for displacements,} \\ M_F(z,t,\omega) = K\sum_{j=1}^{\infty} a_j\frac{\partial\psi_j(z)}{\partial z}\int_0^t h_j(\tau)A(t-\tau,\omega)\mathrm{e}^{-\mathrm{i}\omega\tau}\,\mathrm{d}\tau & \text{for shear forces.} \end{cases} \tag{32}$$

5. Peak structural response

To properly assess the structural response one needs to know estimations of peak response rather than only mean square response derived in the previous section. For stationary random vibrations or the non-stationary ones but still with the duration of excitations much longer than the fundamental natural period the classic peak factors by Davenport [21] or Vanmarcke [22] can be applied with acceptable, though still approximate results. This is, however, not the case for analyzed here vibrations of typical building structures ($0.5\,\mathrm{s} < T_1 < 2\,\mathrm{s}$) under short, 1–2 s high frequency excitation pulses like the rockbursts or similar loads. In this case the peak response can be obtained only by using numerical estimations, e.g. the formulae of Yang [23] who proposed to calculate the first excursion probability of double, symmetric barrier $\pm\lambda$

$$P(\lambda) = 1 - \exp\left[-\int_0^\infty v(\tau,\lambda)\,\mathrm{d}\tau\right] \tag{33}$$

as a function of time dependent failure rate $v(t,\lambda)$:

$$v(t,\lambda) = 2v_+(t,\lambda)\frac{1-\exp[-v_e(t,\lambda)/(2v_+(t,\lambda))]}{1-v_+(t,\lambda)/v_+(t,0)} \tag{34}$$

in which $v_+(t,\lambda)$ stands for mean number of up-crossing level λ by the response process while $v_e(t,\lambda)$ represents respective mean number of crossing level λ by the envelope of the response process. The mean number of crossing level λ with positive slope by the response process $q(t)$ can be obtained using the familiar Rice formula, after integrating the joint probability density of the process $q(t)$ and its derivative $\dot{q}(t)$:

$$v_+(t,\lambda) = \int_0^\infty \dot{q}p_{q\dot{q}}(\lambda,\dot{q};t)\,\mathrm{d}\dot{q}. \tag{35}$$

Assuming in this case two-dimensional standard Gaussian probability density, substituting it to the above equation and carrying out the integration gives

$$v_+(t,\lambda) = \frac{\sigma_{\dot{q}}}{2\pi\sigma_q}\sqrt{1-\rho_{q\dot{q}}^2}\exp\left(-\frac{\lambda^2}{2\sigma_q^2}\right) \times\{\mathrm{e}^{-v^2} + \sqrt{\pi}v[1+\mathrm{erf}(v)]\} \tag{36}$$

in which

$$v = \frac{\lambda\rho_{q\dot{q}}}{\sigma_q\sqrt{2[1-\rho_{q\dot{q}}^2]}}, \quad \sigma_{\dot{q}} = \sigma_{\dot{q}}(t) = \langle\dot{q}^2(t)\rangle,$$
$$\rho_{q\dot{q}} = \rho_{q\dot{q}}(t) = \frac{\langle q(t)\dot{q}(t)\rangle}{\sigma_q(t)\sigma_{\dot{q}}(t)}. \tag{37}$$

A similar analysis can be done for the envelope crossing rate v_e yielding approximate relation:

$$v_e(t,\lambda) = \frac{\lambda\sqrt{\gamma_2-\gamma_1^2/\sigma_q^2}}{\sqrt{2\pi}\sigma_q^2}\exp\left[-\frac{\lambda^2}{2\sigma_q^2}\right], \tag{38}$$

where γ_j are time dependent spectral moments:

$$\gamma_j = 2\int_0^\infty |M(z,t,\omega)|^2[\omega+\dot{\delta}(t,\omega)]^j S_{\ddot{u}}(\omega)\,\mathrm{d}\omega \quad \text{for } j=1,2 \tag{39}$$

and

$$\dot{\delta}(t,\omega) = \frac{\partial}{\partial t}\tan^{-1}\frac{\mathrm{Im}\,M(z,t,\omega)}{\mathrm{Re}\,M(z,t,\omega)}. \tag{40}$$

The peak value can be defined as a value of λ corresponding to respective probability of excursion. For example the median peak value $\lambda_{0.5}$ corresponds to probability of outcrossing domain $\pm\lambda$ with probability 0.5 i.e.:

$$P(\lambda) = 0.5 = 1 - \exp\left[-\int_0^\infty v(\tau,\lambda_{0.5})\,\mathrm{d}\tau\right] \tag{41}$$

in which the unknown median peak value is in the integrand. This equation can only be solved numerically. In an analogy to the Davenport's peak factor [21] one can define the median peak factor as the ratio of median peak value to the maximum rms response i.e.: $r_{0.5} = \lambda_{0.5}/\max\sigma_{0.5}$.

6. Numerical analyses

Consider the shear beam from Fig. 3, with height $H = 35\,\mathrm{m}$. The main parameter which accounts for both elastic and inertial properties of the shear beam is the value of velocity of shear waves propagating along its height, c_S. The values of c_S ranging from 100 to 200 m/s are commonly met in the literature [13–16]. In this paper the value of $c_S = 170\,\mathrm{m/s}$ has been applied. The cantilever beam with such parameters can roughly represent a 10 story, prefabricated building which is usually built with the same cross-section along its height. The first eight natural frequencies and periods were calculated for these values of H and c_S using Eq. (3) and are given in Table 1. In the detailed numerical analyses which follow, formulas (26)–(41) are applied. In all the following calculations the value of damping ratio $\xi = 0.05$, the same for all the modes of the analyzed beam is applied. It is a violation of the modal decoupling requirements but keeping constant damping makes it easier to identify the contributions of various modes regardless of the applied damping

Table 1
The first eight natural frequencies and periods of the analyzed beam with $H = 35\,\mathrm{m}$ and $c_S = 170\,\mathrm{m/s}$

Mode number	1	2	3	4	5	6	7	8
Natural frequency (Hz)	1.21	3.64	6.07	8.50	10.93	13.36	15.79	18.21
Natural period (s)	0.824	0.275	0.165	0.118	0.092	0.075	0.063	0.055

hypothesis. Such assumption is also recommended in the recent paper on shear beam seismic vibrations by Sasani et al. [18]. Nevertheless, as suggested by one of the Reviewers, the effect of the applied damping model on the shear beam response is studied in detail at the end of this chapter (Fig. 10).

To model the characteristic effect of frequency shift in excitations as described earlier (Fig. 2), two frequency bands are considered:

(a) from 1 to 4 Hz (dominating spectrum of earthquakes or rockbursts type II),
(b) from 4 to 16 Hz (high frequency effects of rockbursts type I).

The cut-off frequencies of band-limited white noise can be obtained just by multiplying them by a single "scale" factor $s = 1$ or 4 as required in formula 5 (Fig. 4). It can be seen from Table 1 that in the first case only the first two natural modes will be excited while for the second case only modes 3–7 will contribute in the vibrations.

As the shear beam drift is of our particular interest, the actual shear force response which is a direct function of the drift ($F(z) = K\partial q/\partial z$) will be analyzed here in detail. The value of shear at $z = 0$ plays particular role in seismic engineering as the *base shear*—the approximate seismic force to be distributed along the height of the building being designed. In addition to the base shear, a value of the shear force at $z = 31.5$ m is analyzed more carefully here as it corresponds to the drift of the last floor of the equivalent 10-story building.

To check the basic characteristics of the shear beam response the stationary spectral densities of the shear forces for $z = 31.5$ m and $z = 0$ are shown in Fig. 5a and b, respectively. Substantial domination of the first vibration mode can be seen from this figure. For $z = 31.5$ m the contribution of second, third and fourth modes is slightly more evident. The frequency band 4–16 Hz was also displayed in zoomed in-sets in this figure. It can be seen that for the frequency band limited to the range 4–16 Hz the modes third, fourth, fifth, and sixth (now the first, second,… etc.) do not attenuate as fast as for the low frequency excitations.

Now consider the non-stationary response of the shear beam under band-limited short time, white noise excitations. The duration of excitation was chosen to be 1.5 s, typical for the type I rockbursts and comparable with the first natural period of the analyzed shear beam. In Fig. 6 the evolution of the spectral density of the shear force at $z = 31.5$ m is shown as it changes with time. It can be seen as the response changes from the broad-band at the beginning, to more and more narrow-band as time passes on, particularly after the excitations seized ($t > 1.5$ s). Again, for the frequency band 4–16 Hz (Fig. 6b) the contributions of subsequent modes become more uniform. The early moments of high frequency excitations represent even more broad-band response than for the low frequency

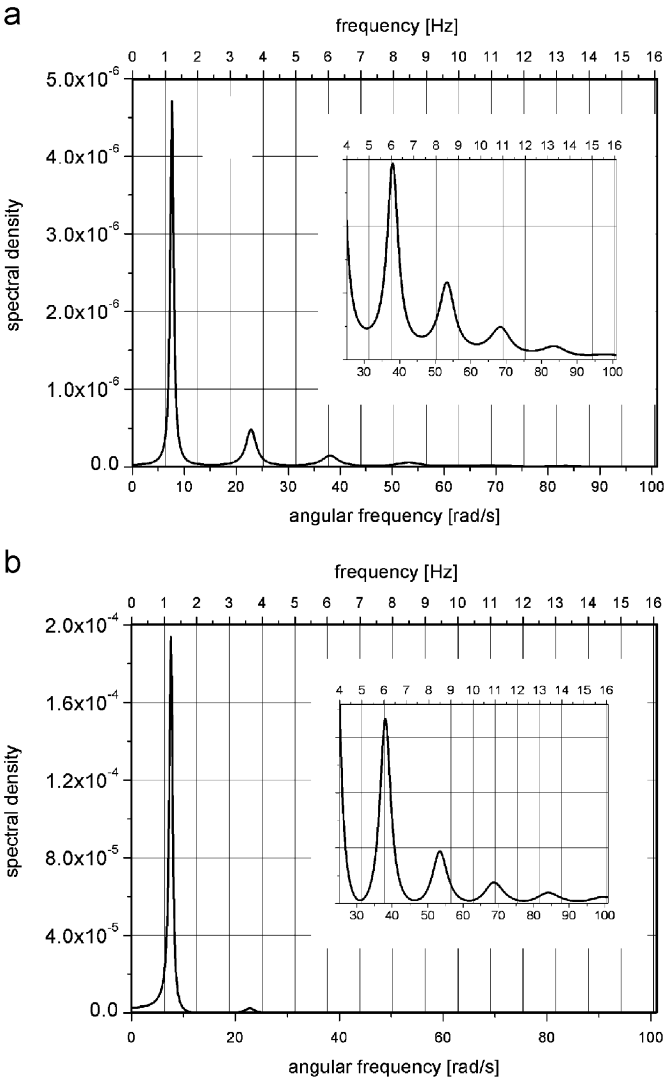

Fig. 5. Spectral density of stationary shear force response at height $z = 31.5$m (a) and $z = 0$ (b) with a zoomed box for frequencies over 25 rad/s.

one. In Fig. 7 the rms shear response is shown for base shear (b, d) and for $z = 31.5$ m (a, c). Figs. 7a,b show the response for the frequency band 1–4 Hz while Figs. 7c,d show the rms shear response for frequency band 4–16 Hz. In all analyzed cases the response gradually increases until $t = 1.5$ s and then slowly decreases, with some oscillations representing the fundamental period of the structure. For the low frequency band (a, b) and such short duration of excitations (1.5 s) the rms response starts to decay well below the stationary response level. However, for the high frequency excitations the non-stationary response reaches its maximum already at the beginning of excitations, substantially overshooting the stationary response level. The median peak factors (Eq. (41)) are higher for the high frequency excitations: $r_{0.5} = 3.75$ for $z = 31.5$ m and 3.77 for $z = 0$. For low frequency excitations these values equal 3.25 and 2.94, respectively. This means that the distribution of peaks is practically the same for base shears and

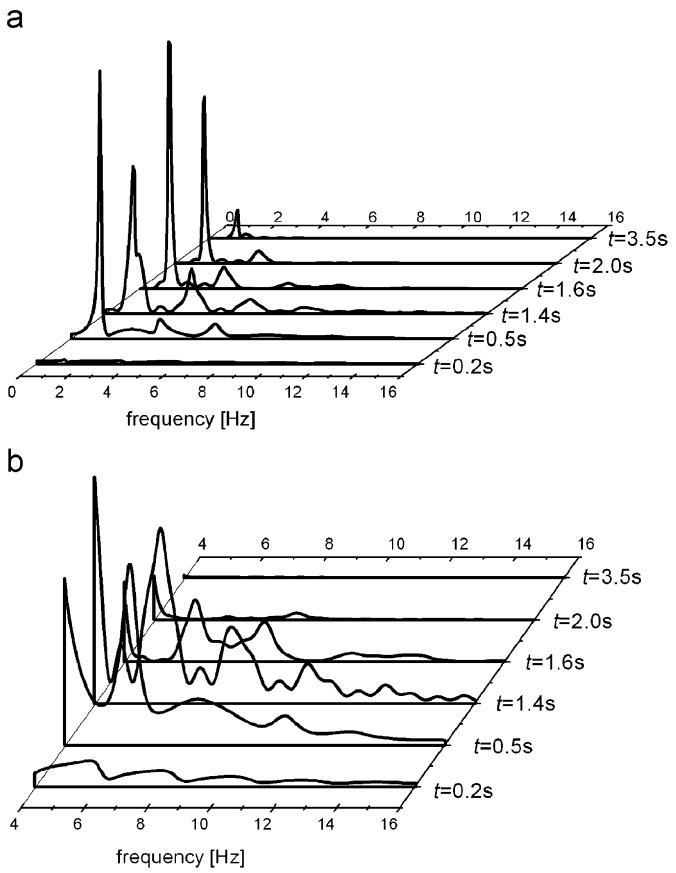

Fig. 6. Spectral density of shear forces evolving with time for $z = 31.5$ m: (a) the whole spectrum band 0–16 Hz; (b) zoom of upper band frequencies 4–16 Hz.

$z = 31.5$ m and generally much wider for the high frequency excitations. In Fig. 8 the probability densities of the first passage time are shown for the base shear responses and low frequency excitations (Fig. 8a) as well as for the high frequency ones (Fig. 8b). Both plots depend first of all on the rms responses, but also on the other parameters of response (rms velocity, correlation: force and its velocity as well as two spectral moments γ_1 and γ_2—Eq. (39)). The maximum response occurs at the end of excitations for the low frequency excitations, so the maximum of probability density occurs also at this moment. When the excitations frequency band is the higher one, the maximum response occurs soon after the beginning. It is reflected in the respective plot of the probability density function. In both cases of the excitations one can observe the fast decrease of the probability density. Such fast decrease of the integrand makes it possible to include only limited duration of response and limits the numerical efforts. In Fig. 9 the maxims of rms non-stationary responses and respective median peak values are shown as functions of z. The stationary rms response level is shown for comparison too. For the assumed criterion of constant peak velocity the high frequency excitations result in smaller response (Fig. 9b) than for the low frequency effects (Fig. 9a). In Fig. 10 the sensitivity of the peak response to assumed damping ratios and models are shown. For mass and stiffness proportional damping the value of the first modal damping ratio was assumed, while the remaining modal damping ratios were calculated according to Eqs. (13) and (14), respectively. As

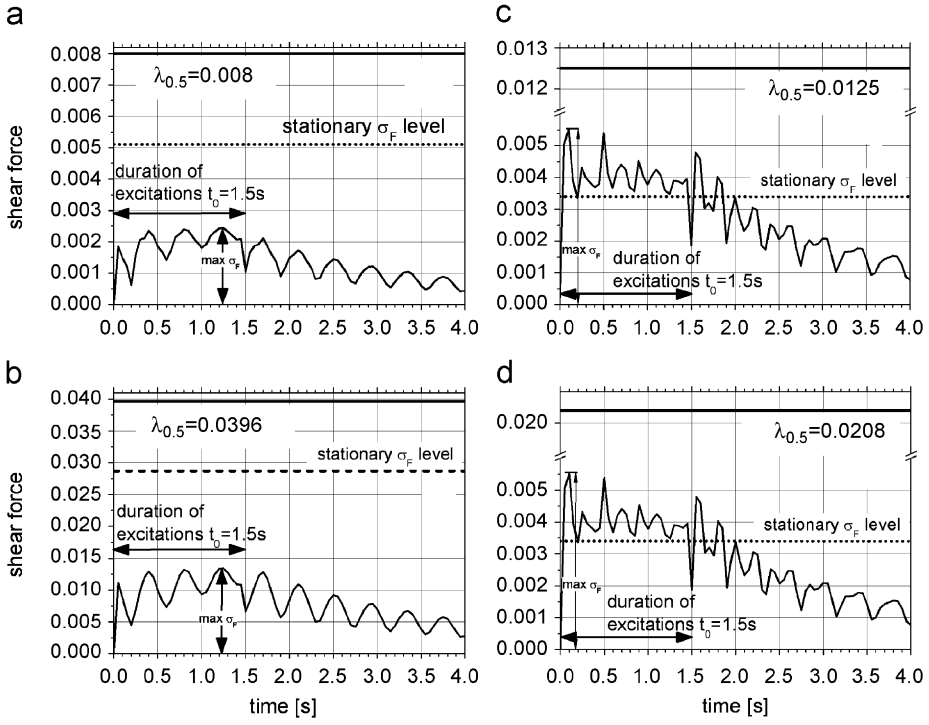

Fig. 7. Rms shear as a function of time for $z = 0$ (base shear—b,d) and $z = 31.5$ m (a,c): low frequency excitations, bandwidth 1–4 Hz—scale factor $s = 1$—(a,b); high frequency excitations, bandwidth 4–16 Hz—scale factor $s = 4$—(c,d).

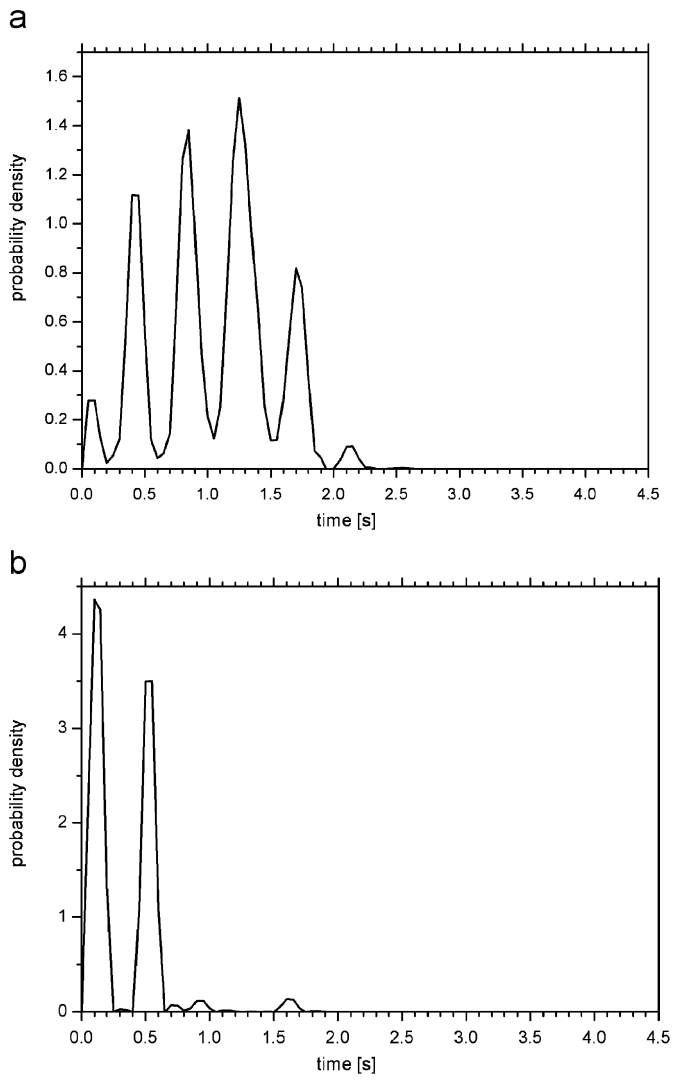

Fig. 8. Probability density of the base shear first passage time for low frequency excitations (a) and for high frequency excitations (b).

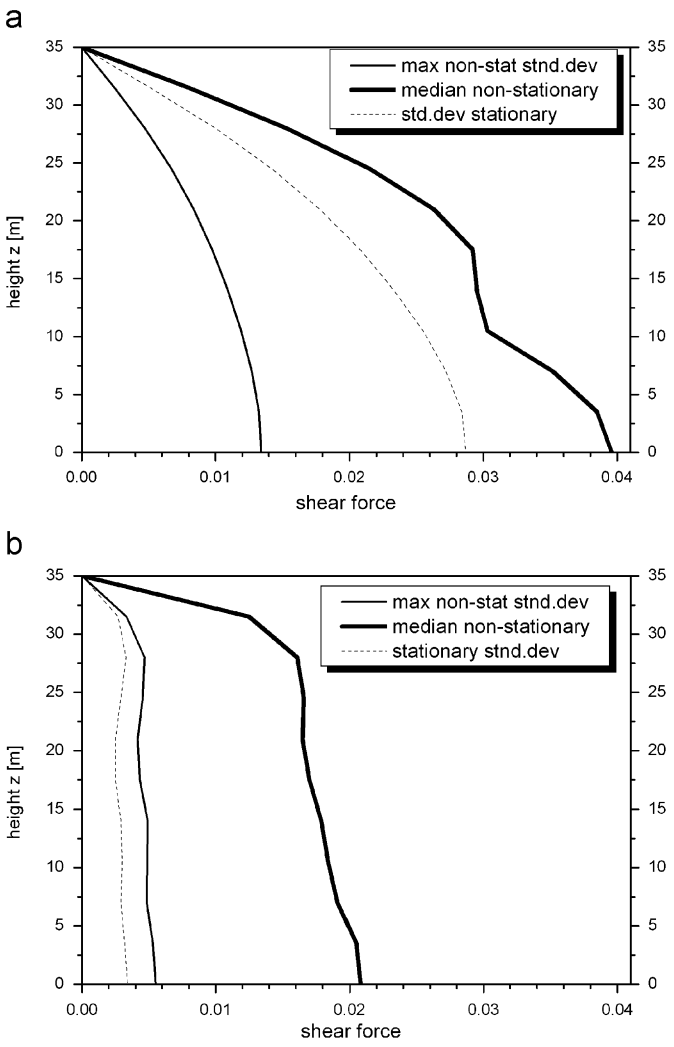

Fig. 9. Max rms shear, median peak value and stationary rms shear as functions of height for: scale factor $s = 1$—spectral bandwidth 1–4 Hz (a,b); scale factor $s = 4$—spectral bandwidth 4–16 Hz (c,d).

could be expected the assumption of stiffness proportional damping gives the lowest response in both cases of low frequency excitations and the high frequency ones. On the other hand the assumption of mass proportional damping gives the highest response in both analyzed cases. When constant modal damping is assumed the structural response under high frequency excitations is less sensitive to the damping variations than the response under conventional, low frequency excitations. However, when looking at the separation between the two applied models the separation between them is much wider when the high frequency excitations are applied. The assumption of stiffness proportional damping results in very low response for most of the range of analyzed damping ratios. It is so because in this case all the modal damping ratios are rather high for all the higher modes.

In Fig. 11 the base shear response is analyzed as a function of the shear beam height. The range of heights from 3.5 to 35 m (single-story to 10-story) corresponds to

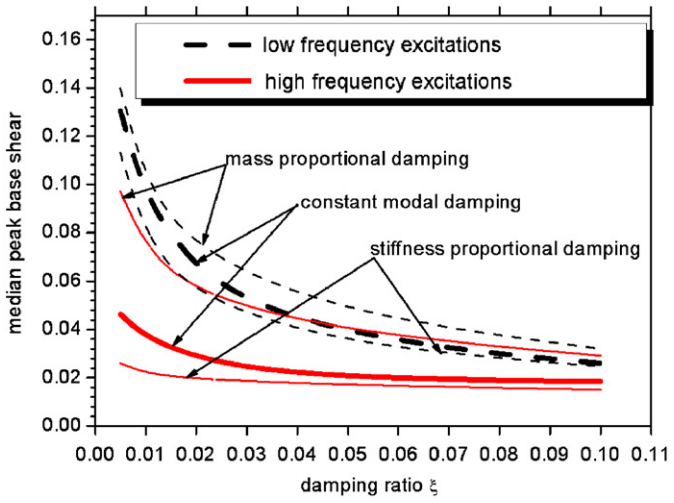

Fig. 10. Effect of damping on median peak response for low frequency excitations (1–4 Hz) and high frequency excitations (4–16 Hz).

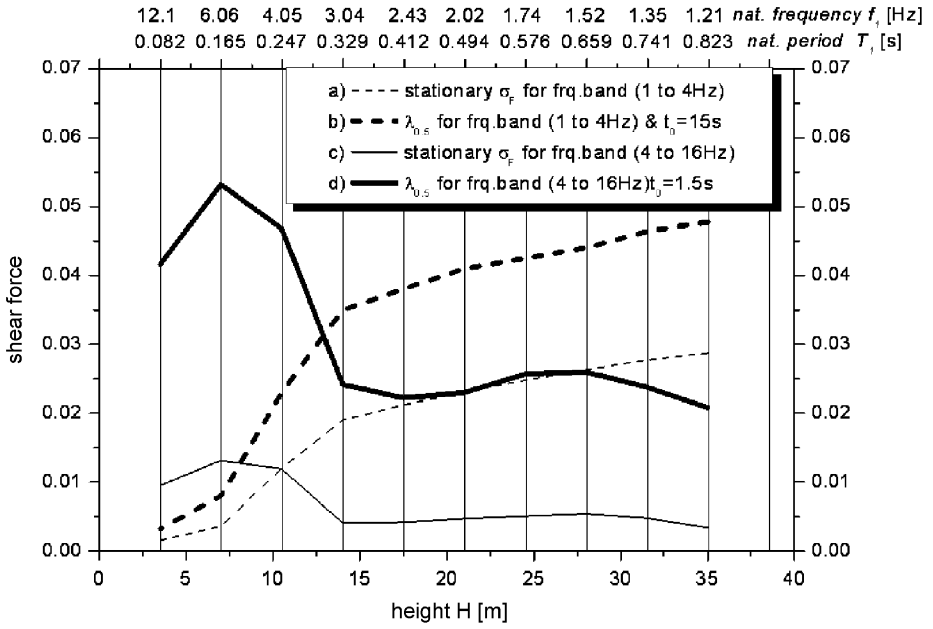

Fig. 11. Base shear force as a function the height and natural frequency of the shear beam (fundamental natural period): (a) stationary standard deviation for low frequency excitations; (b) respective median peak value for low frequency excitations; (c) stationary standard deviation for high frequency excitations; (d) respective median peak value for high frequency excitations.

changes of the first natural frequency from $f_1 = 12.15$ to 1.21 Hz (natural period T_1 from 0.0823 to 0.823 s). To study the effect of low frequency excitations the stationary rms base shear is analyzed in detail (plot a). Since the peak response is a direct function of the elapsed time there is no single number for the stationary median peak value. Thus to compare the stationary response with the short, non-stationary one, the duration of 15 s was chosen to calculate $\lambda_{0.5}$ in this case (plot b). It is long enough to ensure stationarity of response for structures with $T_1 < 1$s. Observing plots (a) and (b) from Fig. 11 one can note an increase of both stationary rms base shear and its respective peak values for low frequency excitations. This increase is particularly prominent for H from 7 to 14 m i.e. for f_1 from 3.04 to 6.06 Hz (T_1 from 0.165 to 0.329 s). However, when it comes to the base shear response to high frequency excitations an opposite effect is observed. For low values of H (3.5–10 m) this response is rather high and then drops down substantially for H greater than 10–15 m that is for f_1 from 3.04 to 4.05 Hz (T_1 0.247–0.329 s). This is an effect of the domination of higher modes in the response for greater values of H. On the other hand, for $H < 15$ m the first modes occur at higher frequencies (4–12 Hz) so they are now excited by high frequency excitations as the principal modes, like during the low frequency excitations. It should be noted, however, that though some increase in the response of low buildings can be observed during high frequency seismic excitations generally these structures sustain the seismic excitations quite well. It is so because the 1–2 story buildings are usually much stiffer than it could be deduced from their shear beam model. The shear beam model is less adequate for these structures than it is for the high buildings due to much stiffer construction of the low buildings. The calculations of seismic response by Finite Element Method and observations of damages during earthquakes and rockburst excitations confirm the above reasoning.

7. Final remarks and conclusions

Short duration, high frequency seismic effects on structures represent specific type of excitations in civil engineering. Critical contribution to the overall seismic structural response is contributed by the frequency band below 5 Hz. A shift in the ground motion Fourier spectrum to higher frequencies results in excitations of higher eigenmodes of the structure. If at the same moment, the excitation spectrum lacks the low frequency band (<5 Hz) then the structural response may substantially be changed. The analysis of a wide range of problems regarding this type of structural dynamics was dealt with in the paper by Lu et al. [7], particularly for very high frequency shifts characteristic to blast ground motion. Present paper aimed at intermediate shift of excitation frequencies (4–16 Hz) and at analyzing non-stationary random vibrations of a shear beam as a simplified model of multistory building. Unlike for the conventional random vibrations which slowly build up and for short excitations their rms values may never reach the respective stationary level before the excitations are seized (Fig. 7a,b), the high frequency effects cause the rms response to almost instantly cross the stationary level, resulting in characteristic over-shoot phenomenon (Fig. 7c,d). When comparing the low frequency vibrations with the high frequency ones (with the same excitation velocities) the conventional seismic excitations result in higher response, but the dominating

contribution of higher modes of vibration results in specific increase of the high frequency response in the upper part of the shear beam (Fig. 9b). For higher frequencies of excitations the structural response is more susceptible to the choice of the damping model. When constant modal damping is assumed the structural response under high frequency excitations is less sensitive to the damping variations than the response under conventional, low frequency excitations. Albeit the low frequency excitations affect more substantially higher buildings, the high frequency effects cause greater shear response to the lower buildings. It should, however, be pointed out that the lower buildings are generally less vulnerable to any dynamic effects as their overall stiffness is greater than for the higher buildings.

Most of the high frequency excitations met in practice do not cause substantial structural damages but evidently affect comfort of people living in the nearby buildings. In addition these high frequency vibrations transmitted from the soil cause particular response of equipment inside the buildings. For example during the rockburst induced vibrations, many cases of falling furniture are reported and are subject of financial compensations by the mine authorities.

References

[1] Ambraseys N, Smit P, Berardi R, Rinaldis D, Cotton F, Berge-Thierry C. Dissemination of European strong- motion data. CD-ROM collection. European Council, Environment and Climate Research Programme, 1999.

[2] Ciesielski R, Maciąg E. Traffic vibrations and their influence on buildings. Warsawk: WKŁ; 1990. p. 1–248 [in Polish].

[3] Juhasova E. Seismic effects on structures. Amsterdam: Elsevier; 1991.

[4] Makris N, Black CJ. Evaluation of peak ground velocity as a "good" intensity measure for near-source ground motions. J Eng Mech ASCE 2004;130(9):1032–44.

[5] Takewaki I. Bound of earthquake input energy. J Struct Eng ASCE 2004;130(9):1289–97.

[6] Veletsos S, Kumar A. Steady-state and transient responses of linear structures. J Eng Mech ASCE 1983;109(5):1215–30.

[7] Lu Y, Hao H, Ma G, Zhou Y. Local-mode resonance and its structural effects under horizontal ground shock excitations. J Sound Vib 2002;254(1):51–68.

[8] Dowding CH. Construction vibrations. London: Prentice Hall; 1996.

[9] Heuze et al. Mine seismicity and the Comprehensive Nuclear-Test-Ban-Treaty, US Department of Energy Report UCRL-ID-132897 or LA-UR-99-384; April 1999, 70pp.

[10] Zembaty Z. Rockburst induced ground motion—a comparative study. Soil Dyn Earthq Eng 2004;24(1):11–23.

[11] Johnston JC. Rockbursts from a global perspective. In: Knoll P, editor. Induced seismicity. Rotterdam, Brookfield: Balkema; 1992. p. 63–78.

[12] Naeim F. The seismic design handbook. 2nd ed. Dordrecht: Kluwer; 2001.

[13] Todorovska MI, Trifunac MD. Antiplane earthquake waves in long structures. J Eng Mech ASCE 1989;115(12):2687–708.

[14] Todorovska MI, Lee VW. Seismic waves in buildings with shear walls or central core. J Eng Mech ASCE 1989;115(12):2669–86.

[15] Safak E. Wave-propagation formulation of seismic response of multistory buildings. J Struct Eng ASCE 1999;125(4):426–37.

[16] Iwan WD. Drift spectrum: measure of demand for earthquake ground motions. J Struct Eng ASCE 1997;123(4):397–404.

[17] Chopra AK, Chintanapakdee C. Drift spectrum vs. modal analysis of structural response to near fault ground motions. Earthquake Spectra 2001;17(2):221–34.

[18] Sasani M, Makris N, Bolt BA. Damping in shear beam structures and estimation of drift response. J Eng Mech ASCE 2006;132(9):851–8.

[19] Clough RW, Penzien J. Dynamics of structures. San Francisco: Prentice-Hall; 1975.

[20] Priestley MB. Power spectral analysis of nonstationary random processes. J Sound Vib 1967;6:86–97.

[21] Davenport AG. Note on the distribution of the largest value of a random function with application to gust loading. Proc Inst Civ Eng 1964;28:187–96.

[22] Vanmarcke EH. On the distribution of the first passage time for normal stationary random processes. J Appl Mech ASME 1975;42:215–20.

[23] Yang J-N. Nonstationary envelope process and first excursion probability. J Struct Mech 1972;1:231–48.